A&A 372, 651–662 (2001)
DOI: 10.1051/0004-6361:20010503

Astronomy & Astrophysics

X–ray emission from the giant molecular clouds in the Galactic Center region and the discovery of new X–ray sources

L. Sidoli[1], S. Mereghetti[2], A. Treves[3], A. N. Parmar[1], R. Turolla[4], and F. Favata[1]

[1] Astrophysics Division, Space Science Department of ESA, ESTEC, Postbus 299, 2200 AG Noordwijk, The Netherlands
[2] Istituto di Fisica Cosmica G. Occhialini, C.N.R., Via Bassini 15, 20133 Milano, Italy
[3] Università degli Studi dell'Insubria, Polo di Como, Dipartimento di Scienze Chimiche, Fisiche, e Matematiche, Via Lucini 3, 22100, Como, Italy
[4] Università di Padova, Dipartimento di Fisica, Via Marzolo 8, 35131, Padova, Italy

Received 19 January 2001 / Accepted 2 April 2001

Abstract. We report the results of X–ray (2–10 keV) observations of the giant molecular clouds Sgr B, Sgr C and Sgr D in the Galactic Center region, together with the discovery of the point-like source SAX J1748.2–2808. The data have been obtained with the MECS instrument on the BeppoSAX satellite. The core of Sgr B2 has an X–ray luminosity of $\sim 6 \times 10^{34}$ erg s^{-1} and its spectrum is characterized by a strong Fe emission line at ∼6.5 keV with an equivalent width of 2 keV. Faint diffuse X–ray emission is detected from Sgr C and from the SNR G1.05–0.15 (Sgr D). A new, unresolved source with a strong Fe line has been discovered in the Sgr D region. This source, SAX J1748.2–2808, is probably associated with a SiO and OH maser source at the Galactic Center distance. If so, its luminosity is 10^{34} erg s^{-1}. We propose that the X–ray emission from SAX J1748.2–2808 is produced either by protostars or by a giant molecular cloud core. Emission from sources similar to SAX J1748.2–2808 could have an impact on the expected contribution on the observed Fe line emission from the Galactic ridge.

Key words. Galaxy: center – ISM: clouds: individual: Sgr B, Sgr C, Sgr D – ISM: supernova remnants: individual: G1.05–0.15 – X–rays: ISM – X–rays: stars: individual: SAX J1748.2–2808

1. Introduction

The Galactic Center (GC) region is characterized by a strong concentration of point-like X–ray sources and by intense diffuse X–ray emission, discovered with the *Einstein* Observatory in the 0.5–4 keV energy range (Watson et al. 1981). The *Ginga* satellite revealed the presence of a 6.7 keV iron line emission from the Galactic plane, particularly bright towards the GC direction (Koyama et al. 1989). The ART–P observations (2.5–30 keV; Sunyaev et al. 1993; Markevitch et al. 1993) showed that the diffuse component follows the distribution of the giant molecular clouds (GMCs hereafter) present in this region. These authors suggested that the diffuse emission is due to scattering in the molecular gas of the X–rays from nearby X–ray binaries. They also predicted the presence of a strong iron line of fluorescent origin at 6.4 keV, that was later observed with the ASCA satellite (Koyama et al. 1996a). Indeed, the high spectral resolution observations performed with ASCA confirmed the presence of the diffuse 6.7 keV line component, extended symmetrically with respect to the GC, and discovered the existence of a diffuse 6.4 keV line. The latter is spatially correlated with the distribution of the molecular clouds and is particularly intense in the direction of the Sgr B2 molecular cloud (Koyama et al. 1996a).

The spectrum of the diffuse emission is well described by a thermal hot plasma with temperature ≥7 keV, but there is also evidence for a multi–temperature, or a non-equilibrium ionization, plasma. In fact, several emission lines are present, with the K–lines from iron and sulfur (at ∼2.4 keV) particularly bright (Koyama et al. 1996a).

The GC X–ray emission is part of the diffuse emission that permeates the Galactic plane (Kaneda 1997; Valinia & Marshall 1998), the nature of which is still unknown. Its temperature is too high to allow the confinement of the emitting plasma by Galactic gravity (Townes 1989); part of it could be due to thermal emission from supernova remnants (SNRs), or to the integrated contribution of discrete weak sources (Watson et al. 1981; Zane et al. 1996), but other emitting processes have been proposed, such as non–thermal emission from SNRs, inverse Compton scattering by relativistic electrons (Skibo & Ramaty 1993),

Send offprint requests to: L. Sidoli,
e-mail: lsidoli@astro.estec.esa.nl

emission lines of non–thermal origin produced during capture of electrons by accelerated ions (Tatischeff et al. 1998), charge exchange by low energy heavy ions with neutral gas (Tanaka et al. 1999), non–thermal emission from the interaction of low energy cosmic ray electrons with the interstellar medium (Valinia et al. 2000).

The 6.4 keV iron line component is thought to be due to irradiation of the clouds by hard photons produced by bright X–ray sources (Koyama et al. 1996a; Murakami et al. 2000; Murakami et al. 2001), located inside or outside the cloud (Fromerth et al. 2001). However, the line emission seems too intense to be due to reprocessing of hard X–rays from any known source (external to the cloud) in the GC region. A possibility for the illuminating source is the GC itself, the putative massive black-hole Sgr A* (Ghez et al. 1998), during a past phase of high-energy activity (Koyama et al. 1996a; Churazov et al. 1996).

We report here on new X–ray observations of three giant molecular clouds of the GC region: Sgr B, Sgr C and Sgr D. The data were obtained during a survey of the GC region performed with the BeppoSAX satellite in 1997–1998. The results on the population of discrete bright sources have been reported elsewhere (Sidoli et al. 1999; Sidoli 2000), while those on the diffuse emission from the Sgr A region can be found in Sidoli & Mereghetti (1999).

2. Molecular clouds in the Galactic Center region

The interstellar medium (ISM) in the inner 500 pc of the Galaxy is dominated by molecular gas (Güsten 1989) mostly contained in giant molecular clouds. These clouds have peculiar properties, compared to those of the Galactic Disk clouds: higher turbulence, higher densities ($\geq 10^4$ cm^{-3}) and higher average kinetic temperatures ($T \sim 70$ K, Hüttemeister et al. 1993). High densities are indeed required against tidal disruption in the gravitational potential of the GC region (Güsten & Downes 1980). The high kinetic temperatures are probably produced by shocks and dissipation of turbulence driven by the differential Galactic rotation (Wilson et al. 1982).

The ISM in the GC environment has been surveyed in a large variety of molecules, each tracing gas with different densities: ^{12}CO (Oka et al. 1998), ^{13}CO (Bally et al. 1987; Heiligman 1987), C^{18}O (Dahmen et al. 1998), CS (Tsuboi et al. 1999), NH_3 (Morris et al. 1983), HCN (Jackson et al. 1996), HNCO and CH_3CN (Bally et al. 1987), SiO (Martin–Pintado et al. 1997; Hüttemeister et al. 1998).

These observations reveal that the GC clouds are mostly distributed at positive Galactic longitudes, display complex kinematic properties and have typical dimensions of ∼10 pc (see Morris & Serabyn 1996 and Mezger et al. 1996 for the most recent reviews). The main molecular clouds in the GC region are Sgr B, Sgr D and Sgr C. Their relative positions are still not well determined and they are collectively named "the Galactic Center molecular clouds complex". This complex has also been surveyed in the radio continuum (e.g. Anantharamaiah et al. 1991; Gray 1994; La Rosa et al. 2000) revealing both thermal and non–thermal emission. The complexity of the observed structures (possibly physically related with these clouds) is outlined in the following subsections.

2.1. Sagittarius B2

The Sgr B2 GMC is located at a projected distance from the GC of ∼120 pc.

Radio continuum observations reveal that Sgr B2 is one of the most active star-forming regions in our Galaxy. It contains about 50 very compact H II regions, each excited by a newly formed single O/B massive star (see Gaume et al. 1995 for a complete census of these regions). The main H II regions inside the Sgr B2 molecular cloud are located in the North–South direction. The principal group of these compact regions is called "Sgr B2 Main complex" (Sgr B2(M)). Also shell–like and cometary–shaped H II regions are present, maybe due to bow shocks produced by O/B stars with a strong wind moving supersonically through the molecular cloud (Van Buren et al. 1990).

Sgr B2, like all the other molecular clouds, has a non–uniform distribution of density and temperature. Different temperature components are present, as well as clumps with density as high as $n_{H_2} \sim 10^6$–10^7 cm^{-3} and size smaller than 0.5 pc. The average parameters of the cloud are: $n_{H_2} \sim 10^5$ cm^{-3}, diameter ∼20 pc, and total mass $M \sim (5$–$10) \times 10^6\ M_\odot$ (Lis & Goldsmith 1991; Numellin et al. 2000).

The Sgr B1 H II region is located South–West of Sgr B2.

2.2. Sagittarius C

A complex of radio structures is present within a few arcminutes from the Sgr C GMC. The name Sgr C indicates both a molecular cloud and a shell–like H II region, located near the South–West edge of the molecular cloud and probably physically related to it (Liszt & Spiker 1995). North of this shell a straight non–thermal filament is present, running perpendicular to the Galactic plane. Another radio filament extending parallel to the Galactic plane seems to start, in projection, from the eastern edge of the H II region.

2.3. Sagittarius D

Different molecular and radio continuum components are present in this region: a GMC marked by the CO molecule ($J = 3$–2 emission); a peak in the CS emission ($J = 5$–4 line); a thermal radio continuum source, the H II region G1.13–0.10; the non–thermal shell of the G1.05–0.15 SNR.

Observations carried out in the above mentioned molecular lines seemed to indicate that the molecular core

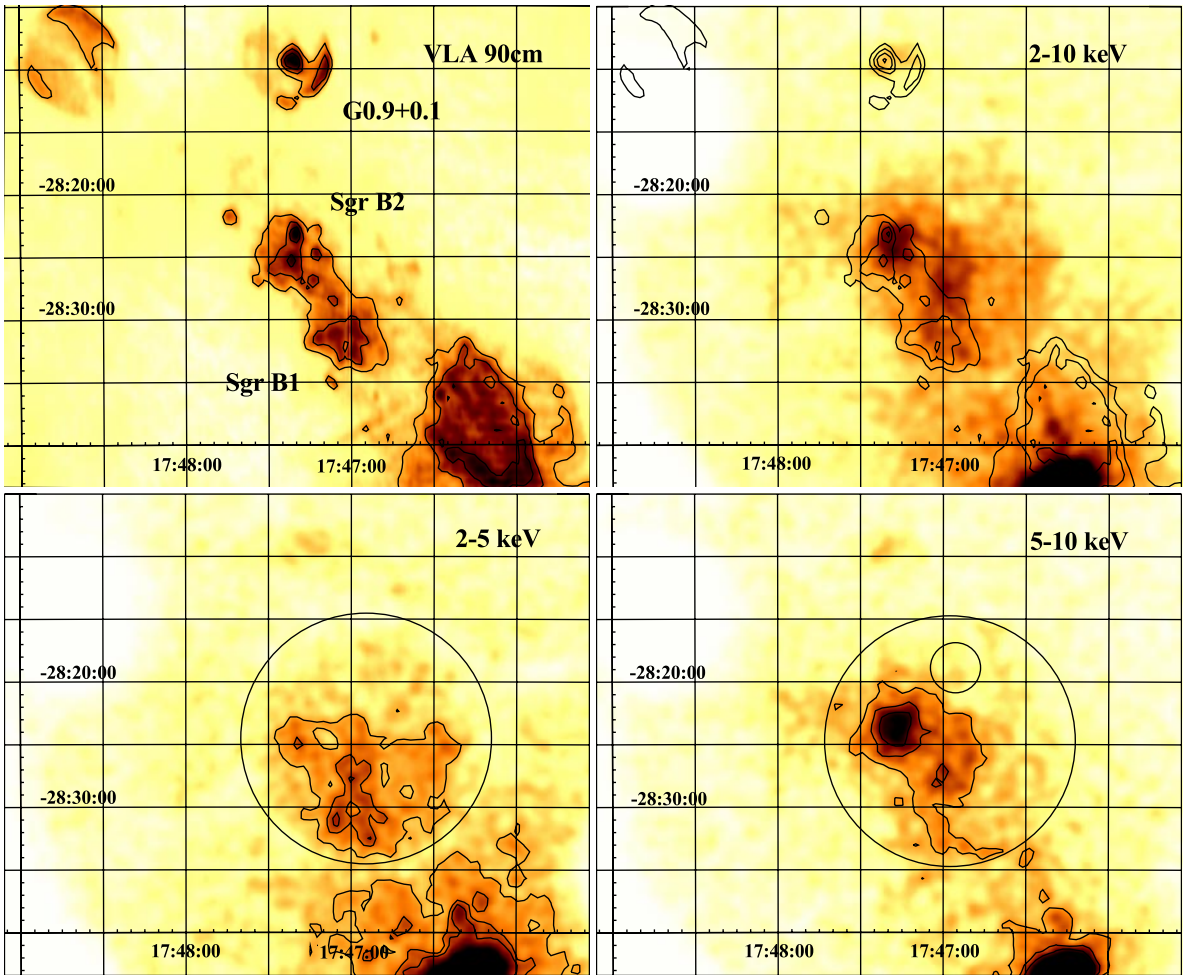

Fig. 1. *Upper panels*: on the left, radio map (VLA, 90 cm; La Rosa et al. 2000) of the Sgr B region. The composite supernova remnant G0.9+0.1 is also visible in the upper part of the region. On the right, MECS image in the total band (2–10 keV) of the same region with the radio contours overlaid. *Lower panels*: soft (2–5 keV; on the left) and hard MECS images (5–10 keV; on the right). The bright source in the lower right of all the X–ray images is the low mass X–ray binary 1E1743.1–2843 (Cremonesi et al. 1999). The smaller circle represents the background extraction region adopted for the Sgr B2 spectral analysis. The larger circle marks the position of the strongback structure of the MECS detector. All the X–ray images have been smoothed with a Gaussian with $FWHM = 1'$. The X–ray contour levels represent 95%, 80% and 60% of the peak intensity. The coordinate grids are in the J2000 equinox.

traced by CS is physically related to the H II region, but not with the molecular cloud traced by the CO line (Lis 1991).

The real location of both the Sgr D H II region and the SNR with respect to the GC is still unclear, although H_2CO observations seem to favor the hypothesis that they are not located at the GC, but beyond it (Lis 1991; Mehringer et al. 1998).

3. Observations and data analysis

The data analysed here were obtained with the MECS instrument (Boella et al. 1997). The MECS operates in the 1.8–10 keV energy range, providing a moderate spatial ($\sim 1'$ full width at half maximum ($FWHM$)) and energy resolution ($\sim$8.5% $FWHM$ at 6 keV) over a circular field of view with a diameter of $56'$. The log of observations is reported in Table 1.

Table 1. BeppoSAX observations summary.

Main Target	Pointing Direction l, b	Observation Date	Exposure (ks)
Sgr B2	0.7, −0.04	1997 Sep. 3–4	47.6
Sgr C	359.4, −0.11	1997 Sep. 16	14.3
Sgr D	1.1, −0.14	1997 Sep. 4–6	45.5

We have not performed a systematic source detection.

In all our spectral analyses, the counts were rebinned to oversample the $FWHM$ of the energy resolution by a factor 3 and to have a minimum of 20 net counts per energy channel, in order to allow use of the χ^2 statistics.

The spectra of the diffuse emission have been corrected with the effective area values appropriate for extended sources, generated with the *effarea* program available in the SAX Data Analysis System (SAXDAS). It convolves a flat surface brightness distribution with the energy and

position dependent vignetting and point spread function. In case of point–like sources, the standard response matrices, appropriate for the extraction regions, have been used.

All the spectra have been corrected for a local background, accumulated from source–free regions of the same observation. All uncertainties are quoted at 90% confidence level.

All fluxes reported in the following sections have been measured within $2'$ from the peak emission, except in the case of Sgr B1 and Sgr D, where more complicated extraction regions enclosed by the radio contours have been considered.

4. Results

4.1. Sagittarius B2

The central part of the MECS (2–10 keV) image pointed on Sgr B2 is displayed in Fig. 1, together with a radio map (90 cm) of the same region obtained with the VLA (La Rosa et al. 2000). In the lower panels of the same figure, the soft (2–5 keV) and hard (5–10 keV) X–ray images are shown. A clear excess, correlated with the spatial distribution of Sgr B2, is present. It is more prominent in the hard X–ray band, while at softer energies there is evidence for X–ray emission from Sgr B1 with a net count rate of $(1.71 \pm 0.11) \times 10^{-2}$ s^{-1} (2–10 keV).

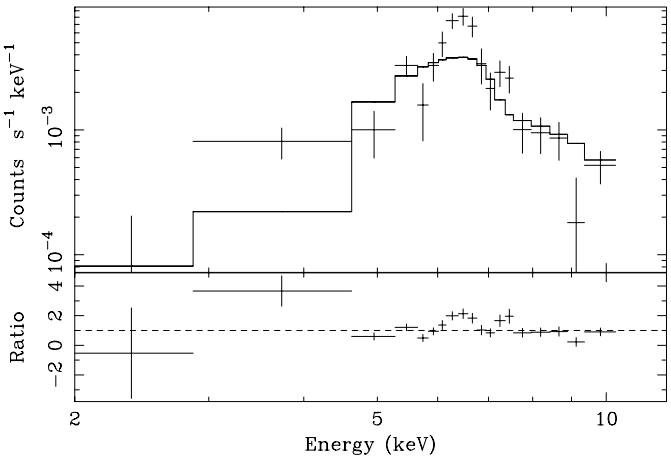

Fig. 2. MECS counts spectrum of the Sgr B2 molecular cloud X–ray emission fitted with a strongly absorbed power-law. Positive residuals at ∼6–7 keV are clearly visible, thus requiring the addition of a Gaussian line to the model.

The peak of the hard X–ray emission from Sgr B2 is at coordinates RA = $17^{\rm h}47^{\rm m}16^{\rm s}$, Dec = $-28°23'40''$ (J2000), consistent, within the position uncertainties (∼$1'$), with that reported by Murakami et al. (2000; ASCA, 6.2–6.6 keV). For the spectral analysis we accumulated counts from a circle with a $2'$ radius centered on this position. The background extraction region is displayed in Fig. 1. We verified that also with other backgrounds, always extracted from source-free regions located inside the strongback structure of the detector, the spectral analysis gave consistent results.

The fit with a single power-law is unacceptable (χ^2/d.o.f. = 62.2/16; d.o.f. = degrees of freedom). It shows both a strong emission line in the 6–7 keV region and a very high absorption at low energy (see Fig. 2). The addition of a Gaussian line results in the following best fit parameters: interstellar absorption $N_{\rm H} = (45^{+45}_{-38}) \times 10^{22}$ cm^{-2}, power-law photon index $\Gamma = 2.0^{+1.5}_{-1.0}$, line energy $E_{\rm line} = 6.50 \pm 0.07$ keV, line equivalent width $EW = (2.0^{+1.1}_{-0.8})$ keV, line intensity $I_{\rm line} = (0.7{-}1.8) \times 10^{-4}$ photons cm^{-2} s^{-1} (χ^2/d.o.f. = 25.1/13). The 2–10 keV (or 4–10 keV) observed flux is $\sim 1.8 \times 10^{-12}$ erg cm^{-2} s^{-1}. The 2–10 keV flux (corrected for absorption) is $F_{\rm X} = 6.9 \times 10^{-12}$ erg cm^{-2} s^{-1}, which corresponds to an X–ray luminosity $L = 5.6 \times 10^{34}$ erg s^{-1}, for a distance of 8.5 kpc. The fit to the spectrum is shown in Fig. 3. There are some positive residuals at 7.4 keV, which are probably caused by an inappropriate modeling of the continuum and/or of the nearby Fe I edge at ∼7.1 keV. In fact the addition of a second Gaussian line is not statistically significant.

Although the fit residuals and χ^2 values suggest that more complex models are probably needed, we performed the following further fits to the data, to allow a comparison with the ASCA results (Murakami et al. 2000).

A power-law plus a Gaussian line with fixed $N_{\rm H}$ (from 10 to 85 $\times$ 10^{22} cm^{-2}) resulted in a photon index ranging from 0.17 to 3.3. The line center was always found at ∼6.5 keV. The line width varied between $\sigma = 240$ eV and $\sigma = 55$ eV and its intensity in the range $\sim(0.9 - 1.7) \times 10^{-4}$ photons cm^{-2} s^{-1}, corresponding respectively to EWs of 1 and 4.5 keV. A fit with a free column density and fixed photon index $\Gamma = 2$, resulted in $N_{\rm H} \sim (40 \pm 15) \times 10^{22}$ cm^{-2}, $E_{\rm line} = (6.50 \pm 0.07)$ keV, $I_{\rm line} \sim 1.1 \times 10^{-4}$ photons cm^{-2} s^{-1}, $\sigma \sim 150$ eV, and an EW of 2.2 ± 0.7 keV. The 2–10 keV and 4–10 keV fluxes corrected for the absorption are 7×10^{-12} erg cm^{-2} s^{-1} and 4.5×10^{-12} erg cm^{-2} s^{-1}, corresponding to $L \sim 5.7 \times 10^{34}$ erg s^{-1} and $L \sim 3.7 \times 10^{34}$ erg s^{-1} respectively.

These results differ from the ASCA ones in the absorbing column density (our value is significantly lower) and in the energy of the line, which is significantly higher compared to the 90% confidence range of 6.35–6.45 keV found with ASCA (Murakami et al. 2000).

We tried also a fit with a power-law plus two Gaussian lines (σ fixed at 0), with energies fixed at 6.4 and 6.7 keV. This fit (χ^2/d.o.f. = 24.7/14) gave $N_{\rm H} = (30^{+40}_{-20}) \times 10^{22}$ cm^{-2} and $\Gamma = 1.40^{+1.70}_{-1.25}$. The EWs for the two iron lines, $EW_{6.4} = 660^{+670}_{-210}$ and $EW_{6.7} = 270^{+215}_{-180}$, are again significantly different from the Murakami et al. (2000) results. Indeed they found that the flux contributed by the 6.7 keV is less than 10% of that from the 6.4 keV line, and that the profile of the line they observe is reproduced by the 6.4 keV line alone. This discrepancy can probably be explained by the choice for the local background. Murakami et al. (2000) subtracted from the main

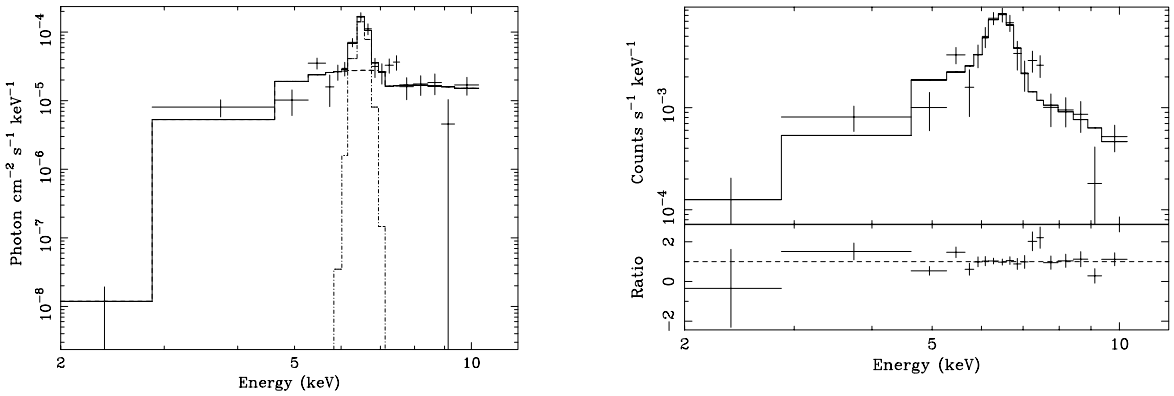

Fig. 3. MECS photon spectrum of the Sgr B2 molecular cloud X–ray emission (left panel) fitted with a strongly absorbed power-law plus a Gaussian line (see the text for details). The count spectrum is shown in the right panel, together with the ratio of observed to model counts.

peak also emission coming from the molecular cloud itself and from the Sgr B1 region (see their Fig. 1), while our choice avoids the region overlapping with the radio contours of both Sgr B2 and Sgr B1.

The final comparison with the ASCA results was performed by extracting the background from the same position used in Murakami et al. (2000). Using their model, an absorbed power-law with the photon index fixed at 2 plus a Gaussian line, we obtained the following results: $N_{\rm H} = (73^{+35}_{-25}) \times 10^{22}$ cm^{-2}, line energy of $6.50^{+0.08}_{-0.09}$ keV, $EW = 1.96^{+2.04}_{-0.77}$ keV (χ^2/d.o.f. = 20.1/12). Thus, in this case, the absorbing column density is compatible with ASCA results. The energy of the iron line is now compatible with the SIS results, but still higher than the GIS 90% confidence range.

We finally tried with another reasonable model for a molecular cloud emitting X–rays: a high temperature plasma model (MEKAL). The fit is unacceptable (χ^2/d.o.f. = 43.8/16), resulting in positive residuals around 6.3 keV ($N_{\rm H} \sim 6 \times 10^{23}$ cm^{-2}; $kT \sim 4$ keV). The addition of a Gaussian line (χ^2/d.o.f. = 25.2/14) at 6.45 keV (6.30–6.55 keV 90% confidence range) resulted in an EW of ∼1 keV and in a temperature $kT \geq 6$ keV with an absorbing column $N_{\rm H} \sim 4 \times 10^{23}$ cm^{-2}.

4.2. Sagittarius C

The X–ray and radio images of Sgr C are compared in Fig. 4. The soft and hard X–ray images (lower panels of Fig. 4) are quite similar. A North–West to South–East excess, with three main peaks, is visible in the total X–ray band. The Northern peak (src 1), located at RA = $17^{\rm h}44^{\rm m}28^{\rm s}$, Dec = $-29°26'15''$ (J2000, ∼1′ error), could be associated with a hot spot in the non–thermal radio filament that ends at the Northern edge of Sgr C (Fig. 4). The central X–ray peak (src 2) is positionally coincident with the Sgr C H II region (RA = $17^{\rm h}44^{\rm m}38^{\rm s}$, Dec = $-29°27'44''$ (J2000)), while the South–Eastern peak (src 3, at RA = $17^{\rm h}44^{\rm m}50^{\rm s}$, Dec = $-29°31'01''$ (J2000)) has no counterparts in the VLA radio map.

Their net count rates in the 2–10 keV energy range are the following: $(6.28 \pm 1.67) \times 10^{-3}$ s^{-1} (src 1), $(1.06 \pm 0.18) \times 10^{-2}$ s^{-1} (src 2, Sgr C H II region) and $(8.94 \pm 1.75) \times 10^{-3}$ s^{-1} (src 3).

4.3. Sagittarius D

Two well defined and contiguous radio shells are evident in the VLA observation (La Rosa et al. 2000) of Sgr D shown in Fig. 5. The Northern shell is the Sgr D H II region (G1.13–0.10), while the Southern one is the supernova remnant G1.05–0.15. The comparison with the MECS image shows weak X–ray emission spatially correlated with some parts of the radio shells, in particular with the Southern rim of the SNR G1.05–0.15 (especially at soft X–ray energies). The MECS count rate from this diffuse structure is $(5.10 \pm 0.79) \times 10^{-3}$ s^{-1} (2–10 keV). If this emission is really associated with G1.05–0.15, this is the first detection of this SNR at X–rays. We note that the emission is statistically significant, but its curved shape is probably an instrumental artifact due to partial absorption caused by the support structure of the detector window, a circular rib (marked by the big circle in Fig. 5) located at ∼10′ from the center of the MECS field of view.

Low surface brightness X–ray emission is also present in the direction of the Sgr D H II region, with a net count rate of $(8.1 \pm 1.1) \times 10^{-3}$ s^{-1} (2–10 keV).

4.3.1. A new source: SAX J1748.2–2808

A point–like X–ray source, without any radio counterpart at 90 cm (see Fig. 5), is visible (particularly in the 5–10 keV image) at RA = $17^{\rm h}48^{\rm m}16^{\rm s}$, Dec = $-28°08'13''$ (J2000, ∼1′ error). This newly discovered source, that we designate SAX J1748.2–2808, has a rather hard and/or strongly absorbed spectrum. The extraction of counts within 2′ from its position yields a net count rate in the 2–10 keV range of $4.84 \pm 0.66 \times 10^{-3}$ s^{-1}. A strong iron line appears to be present in the spectrum of SAX J1748.2–2808. The fit with a power-law plus a Gaussian line led

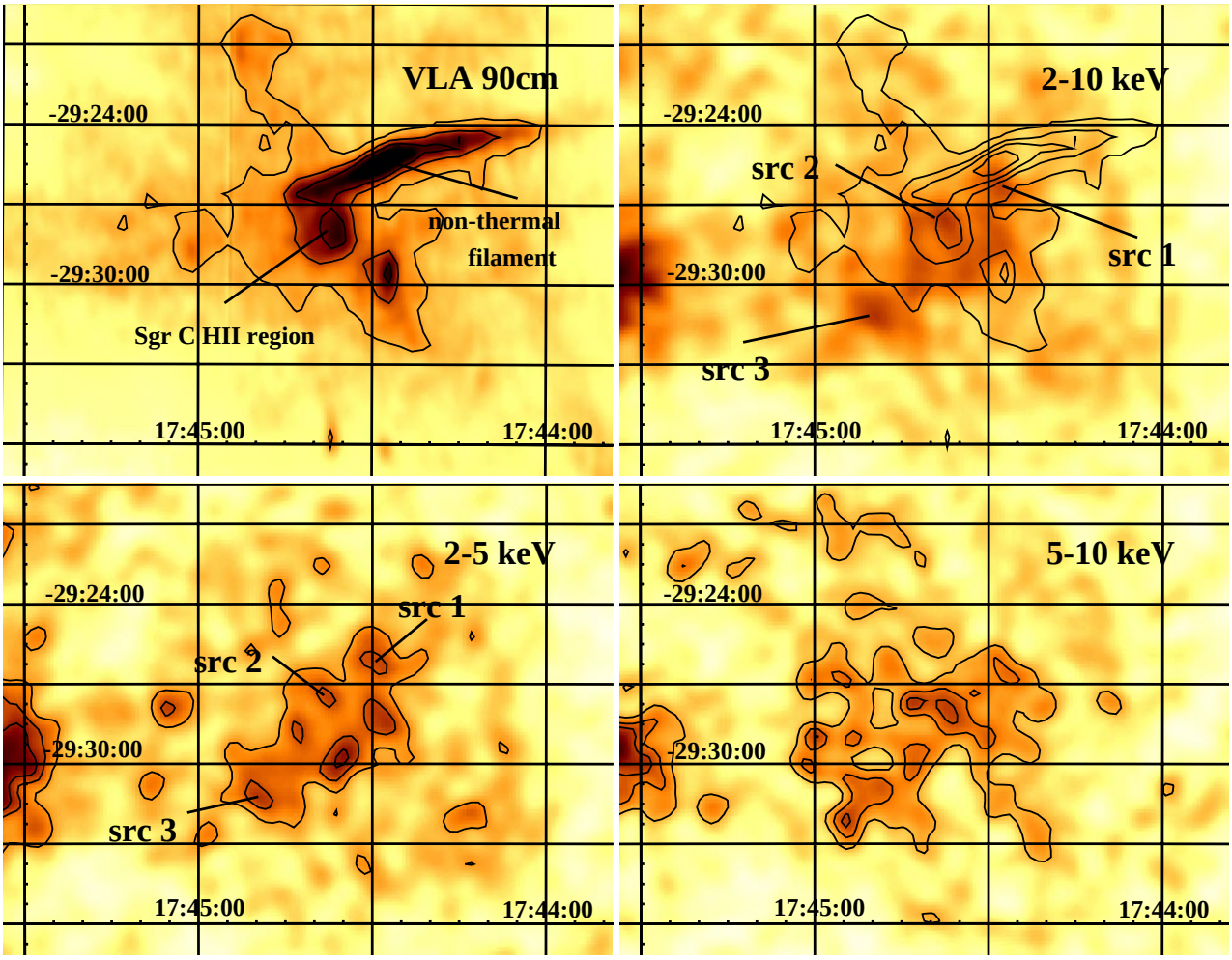

Fig. 4. *Upper panels*: on the left, radio map (VLA, 90 cm; La Rosa et al. 2000) of the Sgr C region. The central blob of radio emission is the Sgr C H II region, while the straight structure is a non–thermal filament running perpendicular to the Galactic plane. On the right, the same region of the sky, imaged with the MECS (2–10 keV) instrument. The radio contours are overlaid for comparison. *Lower panels*: soft (2–5 keV; on the left) and hard MECS images (5–10 keV; on the right). All the X–ray images have been smoothed with a Gaussian with $FWHM = 1'$. The X–ray contour levels represent 95%, 80% and 60% of the peak intensity. The coordinate grids are in the J2000 equinox.

to the following best fit parameters (χ^2/d.o.f. = 3.4/5): $N_{\rm H} = (12^{+15}_{-12}) \times 10^{22}$ cm^{-2}, $\Gamma = 1.9^{+1.7}_{-1.8}$, $E_{\rm line} = 6.62 \pm 0.30$ keV, $EW = 1.2^{+1.0}_{-0.5}$ keV. The 2–10 keV flux corrected for the absorption is $F_{\rm X} = 1.28(^{+1.69}_{-0.54}) \times 10^{-12}$ erg cm^{-2} s^{-1}, corresponding to a 2–10 keV luminosity $L = 10^{34}$ erg s^{-1} (assuming $d = 8.5$ kpc). Taking into account the uncertainty introduced by the poorly constrained spectral parameters, the source luminosity with this model can range from 6×10^{33} to 2.4×10^{34} erg s^{-1} (at 8.5 kpc).

An equally good fit (χ^2/d.o.f. = 4.9/7) was obtained with a thermal equilibrium plasma model (MEKAL in XSPEC) with solar abundance, with the following results: $N_{\rm H} = (13^{+13}_{-6}) \times 10^{22}$ cm^{-2}, $kT = 5.8^{+35}_{-3.7}$ keV, $F_{\rm X} \sim 1.36 \times 10^{-12}$ erg cm^{-2} s^{-1}. The emission measure derived from the normalization of the MEKAL model is $n_{\rm e}^2 V \sim 1.3 \times 10^{57} d_{10}^2$ cm^{-3}, where $n_{\rm e}$ is the electron density, V the emitting volume and d_{10} the source distance in units of 10 kpc. The photon spectrum is displayed in Fig. 6. The absorbing column density in this model translates into an optical extinction $A_V \geq 34$ mag, with a preferred value of $A_V = 73$ mag (Predehl & Schmitt 1995).

Acceptable fits were also obtained with blackbody (χ^2/d.o.f. = 4.0/5) or bremsstrahlung models (χ^2/d.o.f. = 3.5/5) with the addition of a Gaussian line at ∼6.6 keV. In conclusion, the poor statistics does not allow us to discriminate between thermal and non–thermal models for the X–ray emission from SAX J1748.2–2808, even if the presence of an iron line at 6.6 keV favors the thermal hypothesis.

SAX J1748.2–2808 has also been serendipitously detected at large off-axis angle during a MECS observation of the composite SNR G0.9+0.1 (Mereghetti et al. 1998; Sidoli et al. 2000), performed on 1999 August 25–27. Using this observation (net exposure time of 78.5 ks), we derived for SAX J1748.2–2808 a net count rate of $(5.1 \pm 0.4) \times 10^{-3}$ s^{-1} (2–10 keV, corrected for the vignetting). This is compatible with the count rate obtained

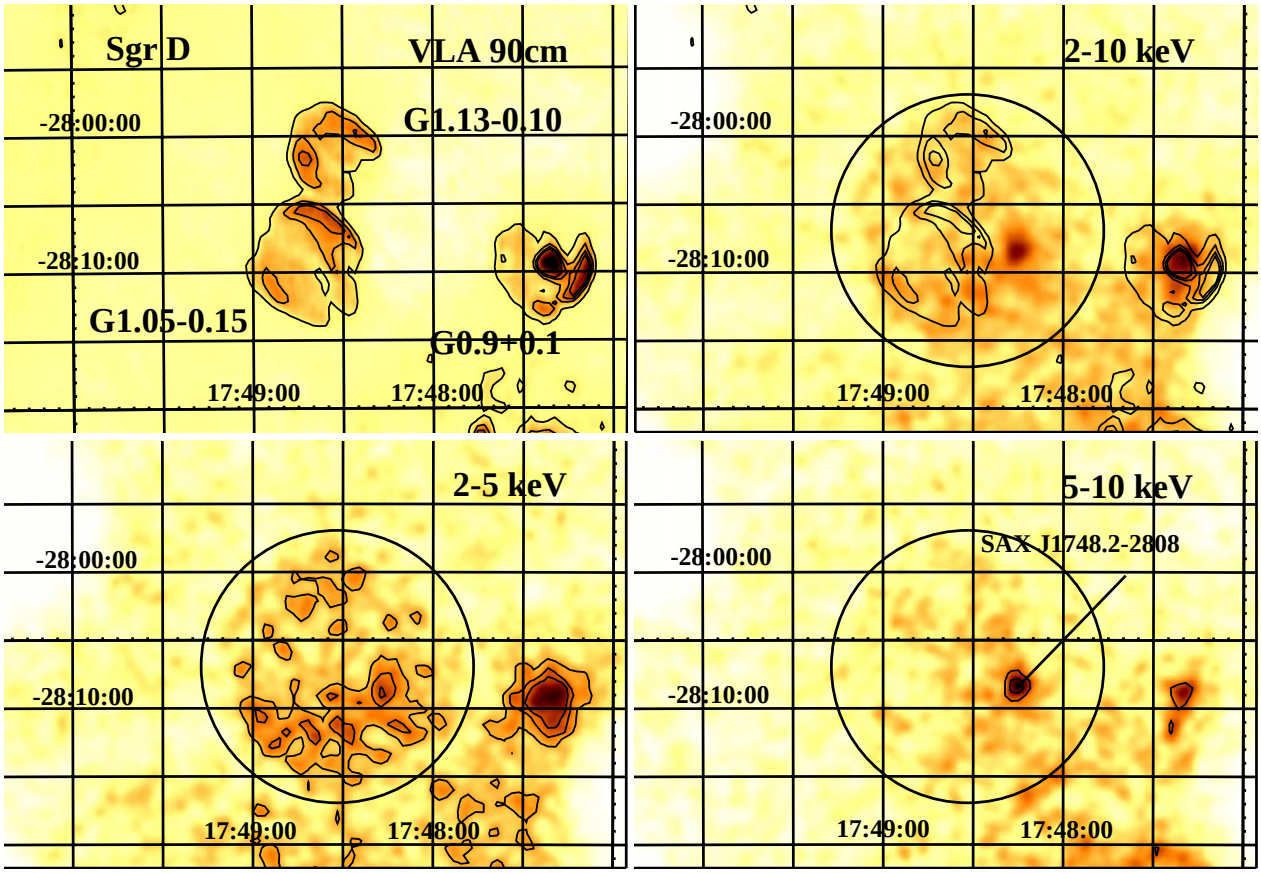

Fig. 5. *Upper panels*: on the left, radio map (VLA, 90 cm; La Rosa et al. 2000) of the Sgr D region. On the right, the same region of the sky imaged with the MECS (2–10 keV) instrument. *Lower panels*: X–ray images, in two energy ranges: soft (2–5 keV) on the left, hard (5–10 keV) on the right. The big circle in the three MECS images represents the position of the circular detector structure of the strongback. All the X–ray images have been smoothed with a Gaussian with $FWHM = 1'$. The X–ray contour levels represent 95%, 80% and 60% of the peak intensity. The coordinate grids are in the J2000 equinox.

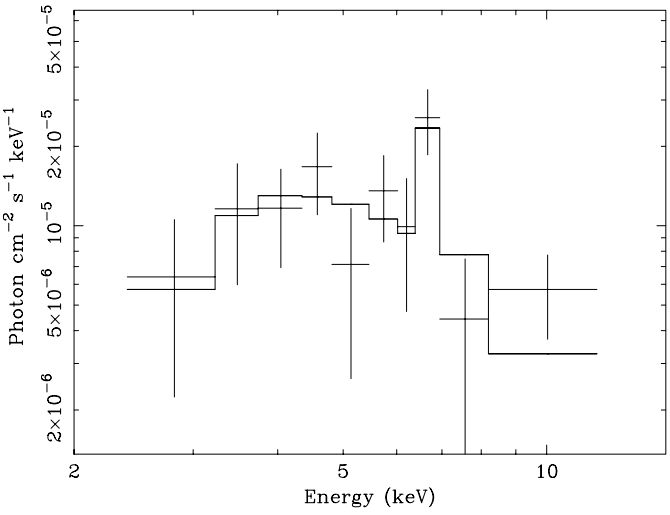

Fig. 6. Observed MECS photon spectrum of SAX J1748.2–2808, together with a MEKAL fit (histogram).

during the Sgr D observation, carried out two years earlier. Thus, SAX J1748.2–2808 does not show evidence for long–term variability. The large off-axis angle prevented us from performing a detailed spectral analysis. All we can say is that, using a power-law plus a Gaussian model and fixing the column density and the power-law index to the best fit results reported above, the 90% confidence ranges for the iron line centroid and the *EW* are: 6.2–7.7 keV and 0.04–1.3 keV. Thus, the iron line emission does not show evidence for variability between the two observations either.

A search in the ASCA public archive resulted in only one observation of the SAX J1748.2–2808 field, performed on 1996 September 19, with an exposure time of ∼22.3 ks. No source can be detected at the SAX J1748.2–2808 position, with a 3σ upper limit of 1.34×10^{-2} s^{-1} (GIS; corrected for the vignetting). This translates into an unabsorbed flux, $F_{\rm X}$, of 2.22×10^{-12} erg cm^{-2} s^{-1} (power-law best-fit model; 2–10 keV), a factor of 1.7 larger than our MECS detection, and thus still compatible with the lack of the long-term variability.

5. Discussion

During the observations of three fields centered on giant molecular clouds in the GC region, we detected X–ray

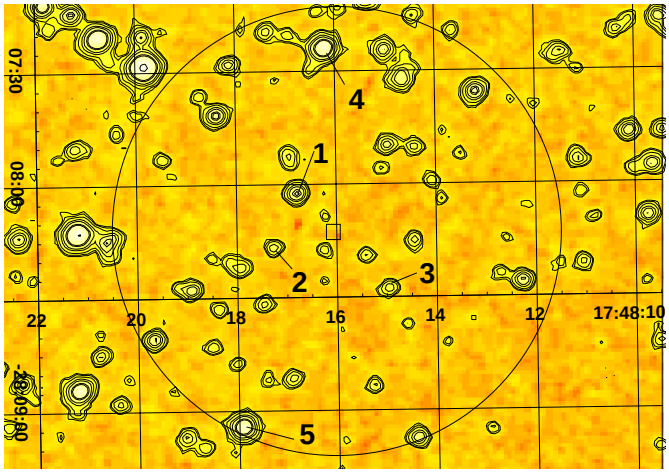

Fig. 7. Optical (red band) image of the uncertainty region of SAX J1748.2–2808. The data are from the "Second Epoch Survey of the Southern Sky" made by the Anglo–Australian Observatory with the UK Schmidt Telescope and provided by the ESO Online Digitized Sky. The large circle marks the MECS error box (1′ radius), the center of which is indicated by the square. The numbers 1, 2 and 3 indicate the three nearest catalogued stars (0.′255, 0.′262 and 0.′330 offset from the X–ray source, respectively). They have the following R and B magnitudes: 16.5 and 18.9 (star No. 1), 17.4 and 20.3 (star No. 2), 17.4 and 20.1 (star No. 3). Numbers 4 and 5 mark the two brightest (in R magnitude) stars inside the X–ray error box; they have R and B magnitudes of 15.2 and 17.2 (star No. 4), 15.3 and 18.0 (star No. 5).

emission from several sources of different kind, both diffuse and point-like. None of them have ROSAT X–ray counterparts (Sidoli et al. 2001).

5.1. A newly discovered point-like source: SAX J1748.2–2808

The optical image of the position of SAX J1748.2–2808, derived from the digitized sky survey provided by ESO/ST-ECF Science Archive is shown in Fig. 7. Eighteen catalogued stars, with R magnitude in the range 15.2–17.4 (and $B \sim 17.2-20.4$), are located inside the X–ray error circle of SAX J1748.2–2808 (1′ radius). The derived optical to X–ray flux ratio $\log(f_{\rm X}/f_{\rm opt})$ is always > -1, thus making an association of SAX J1748.2–2808 with one of these stars unlikely (Maccacaro et al. 1988).

A search in the SIMBAD database resulted in two possible counterparts: the infrared source IRAS 17450–2807 and the SiO maser source SiO 17450–2808 (10″ off-set from the IRAS source), first reported as "object number 6" in the catalogue of SiO maser sources by Shiki et al. (1997). Masers of stellar origin can be excited by radiative or collisional pumping in the outer atmosphere of red (super)giants (Matsuura et al. 2000), around Asymptotic Giant Branch (AGB) stars with large mass loss (Desmurs et al. 2000), or around young stellar objects, where the outflow of material interacts with the surrounding medium (Shepherd & Kurtz 1999).

The SiO maser radial velocity $V_{\rm LSR}$ of +101.2 km s^{-1} is appropriate for a source located in the GC region, thus suggesting a possible association with the Sgr B2 molecular cloud (Shiki et al. 1997). The colors of the infrared source IRAS 17450–2807 make it a likely young stellar object, even if the possibility of a late–type star cannot be completely excluded (Shiki et al. 1997). The IRAS source variability suggests that it could be a Mira–type variable star. A search in the literature resulted in a further maser source coincident (within the positional uncertainties) with SAX J1748.2–2808: a 1667 MHz OH maser source (named "E" in Mehringer et al. 1998) with a velocity of $V_{\rm LSR}$=+75 km s^{-1}. Mehringer et al. (1998) favor the hypothesis that the maser source is associated with an evolved star since it is not spatially correlated with any known H II region. We note that the relatively large uncertainties in their coordinates are consistent with the possibility that these four sources (SiO and OH masers, IRAS source and SAX J1748.2–2808) are the same object.

If the association with the SiO maser source is real, this places the X–ray source at the same approximate distance as the Galactic center, and thus it will have an X–ray luminosity of approx. 10^{34} erg s^{-1}, with an apparently quiescent emission and a rather high temperature of approx. 6 keV. Young stellar objects, and in particular protostars, indeed often have high coronal temperatures, of ≥ 5 keV, even in their non-flaring emission (e.g. as reported by Ozawa et al. 1999 for protostars in Orion), and thus the hypothesis of it being a single protostar would be compatible with the observed spectrum. However, the X–ray luminosity is, specially for a non-flaring source, too high for an individual protostar. While quiescent coronal emission has only been observed in a limited number of protostars, the observed X–ray luminosities seems to be correlated with their mass (see Feigelson & Montmerle 1999), with luminosities limited to few times 10^{31} erg s^{-1} (e.g. Ozawa et al. 1999) at the "low-mass" end (i.e. around a solar mass) ranging to up to $\geq 10^{32}$ erg s^{-1} for more massive protostars (e.g. Nakano et al. 2000).

The X–ray luminosity of SAX J1748.2−2808 is therefore higher than the one of protostars observed up to now. If it indeed the emission is protostellar in origin, the two possibilities are that either it is a protostar more massive than observed up to now in the X–rays, and thus more luminous (assuming that the mass-luminosity correlation extends to higher masses than observed thus far) or that the emission is the result of the superposition of a number (10 or so) high-mass protostars of the type observed by Nakano et al. (2000) in NGC 2264 and which form a compact (and unresolved) cluster. The second hypothesis would be compatible with the observed lack of temporal variability, with the flaring behavior of individual sources likely time-averaged in the ensemble to yield a smooth light curve.

The other possibility is that SAX J1748.2−2808 is the X–ray emission from a giant molecular cloud core (or compact H II region). Emission from H II region cores has been observed with characteristics very similar to the ones of

SAX J1748.2−2808. For example, Hofner et al. (1997) have observed, with ASCA, the core of the W3 region complex, finding a compact (barely resolved) source with an X–ray luminosity of $\simeq 2 \times 10^{33}$ erg s^{-1}. The spectrum shows a visible Fe K line, and it is compatible with being due to thermal emission from a plasma with a temperature of $\simeq$6 keV. In addition to the possibility of emission from a collection of protostars, Hofner et al. (1997) discuss the possibility that the X–ray emission comes from the hot, wind-shocked cavity which is produced by the interaction of the strong stellar wind coming from the more massive stars and the surrounding dense molecular gas. The observed temperature requires wind speeds of about 2000 km s^{-1}, compatible with the wind speeds from massive stars, and the observed X–ray luminosity is compatible with the expected cavity size. This model would thus well explain the emission from SAX J1748.2−2808, and would naturally result in a constant X–ray emission with no flaring activity (as would be common for a protostellar source). More recently, molecular cores with similar X–ray emission, both in terms of temperature and luminosity, have been observed with ASCA in the NGC 6334 giant molecular cloud (Sekimoto et al. 2000).

If indeed the emission from SAX J1748.2−2808 is due to a shocked molecular core cavity, the strong Fe K line observed is apparently more intense than observed in e.g. the W3 core. This could have an impact on the expected contribution of the emission from molecular cores on the observed Fe K line emission in the Galactic ridge (Yamauchi & Koyama 1993). On the basis of the relatively weak Fe K emission observed in the W3 core Hofner et al. (1997) consider that the contribution of molecular cores to the total Fe K ridge emission is likely to not exceed $\simeq$2% of the total. If however the observed stronger Fe K line of SAX J1748.2−2808 is indeed representative of such cores, a significant fraction of the total Fe K ridge emission could effectively be due to them.

We have inspected the maps of the GC region in different molecular lines (e.g., Tsuboi et al. 1999), to look for possible spatial correlation with the position of SAX J1748.2−2808, without finding any convincing association.

Another possibility is that of a nearby stellar object with a strong intrinsic absorption ($N_{\rm H} \sim 10^{23}$ cm^{-2}, that is common among protostars). However this, if the association with the maser sources is real, is in contrast with their high velocity that favors an object located in the GC region.

The X–ray luminosity of SAX J1748.2–2808 (if the assumed distance, also indicated by the high interstellar absorption, is correct) makes an association with an X–ray binary also possible, although the intense iron line emission is unusual for Low Mass X–ray Binaries, where the *EW* is <200 eV, independent from the source luminosity (see e.g. Asai et al. 2000). A different possibility could be a High Mass X–ray Binary (HMXB). A large fraction of HMXBs are accreting pulsars (e.g. van Paradijs 1995). In these systems rather large and highly variable *EW*s (up to 1.8 keV) for the fluorescent Fe K line have been observed (e.g. GX301–2, Leahy et al. 1989). However, flux modulations on the spin and orbital period should be detected as well. Although a spin modulation cannot be ruled out due to the poor statistics, the absence of long-term flux variability does not favor the possibility that SAX J1748.2–2808 is an X–ray pulsar. However, the huge interstellar absorption (>34 mag) prevent us from excluding the presence of a high mass companion star.

The possibility that SAX J1748.2–2808 is a cataclysmic variable should also be considered. X–ray emission from white dwarves can usually be fitted with thermal bremsstrahlung models with temperatures in the range 1–5 keV (Cordova 1995), but also harder spectra are observed (Yoshida et al. 1992). They have luminosity up to 10^{33} erg s^{-1} and K_α iron lines. Both the energy of the Fe line and the temperature of the spectrum match this hypothesis. The observed flux would in this case indicate a distance of only 3 kpc, which is difficult to reconcile with the high absorption.

The possible association with a background AGN is also unlikely, due to the large *EW* of the iron line (typical ranges for Fe K lines *EW*s are 100–500 eV; see e.g. Nandra 2000).

In order to explore the possibility of its association with the Sgr D SNR, we calculated the lower limit $t_{\rm travel}$ to the time required by the neutron star to travel from the center of Sgr D SNR to its present position, about 5–6′ away. This can be expressed by $t_{\rm travel} = 1.4 \times 10^5 \times (d_{10}/v_2)$ yr, where d_{10} is the source distance expressed in units of 10 kpc, and v_2 is the neutron star velocity, in units of 100 km s^{-1}. We can compare this time with the age $t_{\rm shell}$ of the Sgr D SNR as derived from a Sedov solution, using the dimensions of the radio shell (radius of about 4–5′). In this framework, $t_{\rm shell} = 11\,000 \times (n_{\rm ISM}/E_{51})^{1/2} \times (d_{10})^{5/2}$ yr (using a 5′ shell radius), where $n_{\rm ISM}$ is the interstellar medium density in units of cm^{-3}, and E_{51} is the energy of the supernova explosion, in units of 10^{51} erg. If we reasonably assume $d_{10} = 1$, $v_2 = 1$, $n_{\rm ISM}/E_{51} = 1$, then we get $t_{\rm travel} = 1.4 \times 10^5$ yr for the neutron star travel time, and about $t_{\rm shell} = 11\,000$ yr for the adiabatic expansion of the SNR shell, an order of magnitude difference. Alternatively, equating these two times ($t_{\rm travel} \sim t_{\rm shell}$), and assuming the Galactic Center distance and $E_{51} = 1$, we need a very high velocity for the neutron star (velocity = 1400 km s^{-1}; assuming $n_{\rm ISM} = 1$) or a high density environment ($n_{\rm ISM} = 200$, assuming $v_2 = 1$), or, more realistically, v_2 in the range 2–4 (200–400 km s^{-1}) and $n_{\rm ISM} \sim 15$−50 cm^{-3}. Thus, a physical connection with Sgr D SNR is a possibility, but up to now no isolated neutron stars have been observed to show such an intense Fe K line emission. The observability of X–ray emission lines from the surface of magnetized neutron stars seems indeed to be unlikely (Yahel 1982).

In conclusion, we favor the hypothesis that the SAX J1748.2–2808 X–ray emission is produced by protostars (a collection of them or a single high luminosity object) located at the GC distance, or by a giant molecular

cloud core (or compact H II region) shocked by the strong stellar wind coming from the more massive stars.

5.2. X–ray emission from molecular clouds

Molecular clouds can emit X–rays in different ways. In several cases the emission is produced in the star-forming regions naturally located inside the clouds. Pre–main sequence stars are strong X–ray emitters (up to $10^{30}-10^{31}$ erg s^{-1}) with a large variety of behaviors, showing both persistent thermal emission and hard flares (e.g. Koyama et al. 1996b). The *Ginga* satellite provided the first evidence that pre–main sequence stars emit X–rays above 4 keV. Observing the ρ Ophiuchi cloud star-forming region, rich in T Tauri stars and embedded infrared sources, Koyama et al. (1992) obtained a best fit spectrum with a thermal plasma model with $kT \sim 4.1$ keV and an emission line from He-like iron at 6.6 keV. The ASCA satellite revealed that T Tauri stars, and embedded infrared sources with no optical counterparts, can emit X–rays also above 8 keV, with luminosities ranging from 10^{29} erg s^{-1} to 10^{31} erg s^{-1} (reaching 10^{32} erg s^{-1} during flares). These observations also confirmed the important fact that hard X–ray emission can be produced by pre–main sequence stars not only during flares (Koyama et al. 1994).

In the previous section we discussed the nature of a newly discovered X–ray source, finding that its association with several young stellar objects is a likely possibility. It is possible that also the emission from the molecular core of Sgr B2 might be due to several (5–6) objects of the same kind of SAX J1748.2–2808.

Another possibility is the emission from old isolated neutron stars (ONS) accreting from the dense ISM inside the molecular cloud (see e.g., Treves et al. 2000). The possibility that the integrated luminosity from many ONSs might be, at least in part, responsible for the diffuse X–ray emission from the GC region was first suggested by Zane et al. (1996; see also Pfahl & Rappaport 2000 for a recent investigation of X–ray emission from accreting ONSs in globular clusters). Here we follow their approach in evaluating the expected flux produced by accrecting ONSs inside the Sgr B2 cloud. The X–ray luminosity contributed by a single ONS depends on the density $n_{\rm cloud}$ of the molecular cloud and on the relative velocity v of the neutron star with respect to the accreting matter: $L_{\rm ONS} \sim 0.7 \times 10^{33}\ (n_{\rm cloud}/10^4)\ (v/100)^{-3}$ erg s^{-1}. We assume that the spatial and velocity distributions of ONSs follow that of low-mass stars near the GC: $n_{\rm ONS} \sim 4 \times 10^3\ r^{-1.8}$ pc^{-3} and $f(v) \propto (v^2/\sigma_v^3) \exp -(3v^2/2\sigma_v^2)$, where r is the distance from the GC, and σ_v is the velocity dispersion. The monochromatic flux is given by $F_\nu \sim V_{\rm cloud}\ n_{\rm ONS} \int f(v)(\mathrm{L}_\nu/4\pi\, D^2)\mathrm{A}_\nu\, \mathrm{d}v$, where $V_{\rm cloud}$ is the cloud volume, A_ν the interstellar absorption and L_ν the monochromatic luminosity of the single source. The latter is taken to coincide with that produced by a blackbody emitter at the star effective temperature, $T_{\rm eff} \sim 3(L_{\rm ONS}/10^{33})^{1/4} f^{-1/4}$ keV, where f is the fraction of the star surface covered by accretion. For the relevant values of the parameters, $n_{\rm cloud} \sim 10^5$ cm^{-3}, $\sigma_v \sim 75$ km s^{-1}, cloud radius ~ 10 pc, the spectrum peaks around ~ 5 keV, assuming $f = 0.01$, with a total flux of about 4×10^{-12} erg cm^{-2} s^{-1}, close to the observed one. Larger values of f result in softer spectra which are much more severely absorbed ($N_{\rm H} \sim 10^{24}$ cm^{-2} in the present case) and fail to produce the observed flux. The total number of ONSs in the cloud is ∼200, and the typical luminosity for a single source is $\sim 2 \times 10^{34}$ erg s^{-1} which gives an absorbed flux of $\sim 2 \times 10^{-14}$ erg cm^{-2} s^{-1}. Despite the very large ISM density the Thomson depth within the cloud is $\tau_{\rm T} \lesssim 1$, so the emission does not come from a photospheric region. The presence of a large number of discrete sources of hard photons is not in contrast with the finding that most of the interstellar gas is neutral. The Strömgren radius, in fact, is given by $R_{\rm S} \sim 3 \times 10^{15} (n_{\rm cloud}/10^4)^{-5/12} (v/100)^{-3/4} f^{1/12}$ cm (see Blaes et al. 1995 for a thorough discussion), much smaller than the average ONS separation, $\sim n_{\rm ONS}^{-1/3} \sim 10^{18}$ cm.

Molecular clouds can also be the site of reprocessing, scattering and reflection of hard photons from X–ray sources located inside or outside the clouds themselves. The strong X–ray emission in the 6.4 keV line from Sgr B2 has been explained by Koyama et al. (1996a) and by Sunyaev & Churazov (1996) with the reflection of hard X–rays coming from the GC during a past outburst from Sgr A*. Also our data require the addition of a 6.4 keV line to better fit the spectrum from Sgr B2, but we cannot claim the prevalence of the 6.4 keV fluorescent line with respect to the 6.7 keV iron line as in Murakami et al. (2000). It is interesting to note that X–ray emission from ONSs might have the right properties to explain the observed fluorescent iron line. If the source of hard photons is embedded in the cloud, the luminosity required to produce the flux in 6.4 keV line reported by Koyama et al. (1996), $F_{6.4} \sim 1.7 \times 10^{-4}$ photons cm^{-2} s^{-1}, is given by $L_8 \approx 10^{36}\ (0.1/\tau_{\rm T})$ erg s^{-1}, where L_8 is the source luminosity at 8 keV in the 8-keV-wide energy band (Sunyaev & Churazov 1998). Accreting ONSs emit $\sim 1.5 \times 10^{35}$ erg s^{-1}, about 10% of the their total (unabsorbed) luminosity, in the same band. Since the Thomson depth in Sgr B2 is ∼0.7, this is in gross agreement with the required value, taking into account that the cloud material absorbs up to ∼50–60% of the radiation at those energies. Emission of continuum photons inside the cloud together with the derived value of the scattering depth also provides an estimate of the 6.4 keV line equivalent width, $EW \sim \tau_{\rm T} \sim 0.7$ keV (see again Sunyaev & Churazov 1998), which is close to the observed one.

6. Conclusions

The BeppoSAX survey of the Giant Molecular Clouds Sgr B, Sgr C and Sgr D in the GC region has allowed the detection of diffuse X–ray emission from several radio sources, and the discovery of an unresolved source,

SAX J1748.2–2808, probably associated to a group of young stellar objects also observed as an IRAS and maser source, or to a wind-shocked giant molecular core.

Sgr B2 is the strongest diffuse X–ray source. Our spectral results are slightly different from those previously reported by Koyama et al. (1996a). This can probably be ascribed to the different spatial and spectral resolution of the instruments, as well as to the differences in the background subtraction. We also provide an alternative explanation for the X–ray emission from the Sgr B2 molecular cloud, in terms of accretion of the dense molecular cloud matter on the surface of old isolated neutron stars. This scenario can explain the observed luminosity from Sgr B2, as well as the 6.4 keV iron line emission, if the accretion takes place on a small fraction of the neutron stars surface, suggesting the presence of a non negligible magnetic field in old neutron stars.

We detected X–rays also from the H II regions in Sgr D and Sgr C, and from part of the non–thermal radio filament in the Sgr C. Unfortunately, a detailed spectral study of these features is not possible with the limited statistics of the present data. All we can say is that the emission spatially correlated with the radio structures is more prominent in the soft band below 5 keV. The X–rays from H II regions could be explained as the integrated emission from many protostars embedded in these star-forming regions.

Finally, we detected emission spatially correlated with the Southern rim of the SNR G1.05–0.15 in Sgr D. If confirmed, this is the first detection in the X–ray range for this SNR.

Acknowledgements. The BeppoSAX satellite is a joint Italian-Dutch programme. L. Sidoli acknowledges an ESA Research Fellowship. We thank Silvano Molendi and Giorgio Matt for help with the data analysis, Fulvio Melia, Michael Fromerth and Tim Oosterbroek for interesting discussions. We are grateful to Joseph Lazio for providing the VLA radio data. This research has made use of the ESO/ST-ECF Science Archive (available at `http://archive.eso.org`), of the SIMBAD database operated at Centre de Données astronomiques in Strasbourg, and of the High Energy Astrophysics Science Archive Research Center Online Service, provided by the NASA/Goddard Space Flight Center.

References

Anantharamaiah, K. R., Pedlar, A., Ekers, R. D., & Goss, W. M. 1991, MNRAS, 249, 262
Asai, K., Dotani, T., Nagase, F., & Mitsuda, K. 2000, ApJ, 131, 571
Bally, J., Stark, A. A., Wilson, R. W., & Henkel, C. 1987, ApJS, 65, 13
Blaes, O., Warren, O., & Madau, P. 1995, ApJ, 454, 370
Boella, G., Chiappetti, L., Conti, G., et al. 1997, A&AS, 122, 327
Churazov, E., Gilfanov, M., & Sunyaev, R. A. 1996, ApJ, 464, L71
Cordova, F. A. D. 1995, in X–ray Binaries, ed. W. H. G. Lewin, J. van Paradijs, & E. P. J. van den Heuvel (Cambridge Univ. Press), 331
Cremonesi, D. I., Mereghetti, S., Sidoli, L., & Israel, G. L. 1999, A&A, 345, 826
Dahmen, G., Huttemeister, S., Wilson, T. L., & Mauersberger, R. 1998, A&A, 331, 959
Desmurs, J. F., Bujarrabal, V., Colomer, F., & Alcolea, J. 2000, A&A, 360, 189
Feigelson, E. D., & Montmerle, T. 1999, ARA&A, 37, 363
Fromerth, M. J., Melia, F., & Leahy, D. A. 2001, ApJ, 547, L129
Gaume, R. A., Claussen, M. J., De Pree, C. G., et al. 1995, ApJ, 449, 663
Ghez, A. M., Klein, B. L., Morris, M., & Becklin, E. E. 1998, ApJ, 509, 678
Gray, A. D. 1994, MNRAS, 270, 835
Güsten, R., & Downes, D. 1980, A&A, 87, 6
Güsten, R. 1989, in The physics and chemistry of interstellar molecular clouds – mm and sub-mm observations in astrophysics, Proc. of the Symposium, Zermatt, Switzerland, Sept. 22–25, 1988 (A90-33833 14-90) (Berlin and New York, Springer-Verlag), 163
Heiligman, G. M. 1987, ApJ, 314, 747
Hofner, P., & Churchwell, E. 1997, ApJ, 486, L39
Hüttemeister, S., Dahmen, G., Mauersberger, R., et al. 1998, A&A, 334, 646
Hüttemeister, S., Wilson, T. L., Bania, T. M., & Martin-Pintado, J. 1993, A&A, 280, 255
Jackson, J. M., Heyer, M. H., Paglione, T. A. D., & Bolatto, A. D. 1996, ApJ, 456, L91
Kaneda, H., Makishima, K., Yamauchi, S., et al. 1997, ApJ, 491, 638
Koyama, K., Awaki, H., Kunieda, H., et al. 1989, Nature, 339, 60
Koyama, K., Asaoka, I., Kuriyama, T., et al. 1992, PASJ, 44, L255
Koyama, K., Maeda, Y., Ozaki, M., et al. 1994, PASJ, 46, L125
Koyama, K., Maeda, Y., Sonobe, T., et al. 1996a, PASJ, 48, 249
Koyama, K., Hamaguchi, K., Ueno, S., et al. 1996b, PASJ, 48, L87
La Rosa, T. N., Kassim, N. E., Lazio, T. J. W., et al. 2000, ApJ, 119, 207
Leahy, D. A., Matsuoka, M., Kawai, N., & Makino, F. 1989, MNRAS, 237, 269
Lis, D. C. 1991, ApJ, 379, L53
Lis, D. C., & Goldsmith, P. F. 1991, ApJ, 286, 232
Liszt, H. S., & Spiker, R. W. 1995, ApJSS, 98, 259
Maccacaro, T., Gioia, M. I., Wolter, A., et al. 1988, ApJ, 326, 680
Markevitch, M., Sunyaev, R. A., & Pavlinsky, M. 1993, Nature, 364, 40
Martin–Pintado, J., de Vicente, P., Fuente, A., & Planesas, P. 1997, ApJ, 482, L45
Matsuura, M., Yamamura I., Murakami H., et al. 2000, PASJ, 52, 895
Mehringer, D. M., David, M., Goss, W. M., et al. 1998, ApJ, 493, 274
Mereghetti, S., Sidoli, L., & Israel, G. L. 1998, A&A, 331, L77
Mezger, P. G., Duschl, W. J., & Zylka, R. 1996, A&AR, 7, 289
Montmerle, T., Grosso, N., Tsuboi, Y., Koyama, K., et al. 2000, ApJ, 532, 1097
Morris, M. & Serabyn, E. 1996, ARAA, 34, 645
Morris, M., Polish, N., Zuckerman, B., & Kaifu, N. 1983, AJ, 88, 1228

Murakami, H., Koyama, K., Sakano, M., et al. 2000, ApJ, 534, 283
Murakami, H., Koyama, K., Tsujimoto, M., et al. 2001, ApJ, in press [astro-ph/0012310]
Nakano, M., Yamauchi, S., Sugitani, K., et al. 2000, PASJ, 52, 437
Nandra, K., 2000, in proc. of X–ray Astronomy '99 Stellar Endpoints, AGN and the Diffuse Background, Bologna 1999, in press [astro-ph/0007356]
Numellin, A., Bergman, P., Hjalmarson, A., et al. 2000, ApJS, 128, 213
Oka, T., Hasegawa, T., Sato, F., Tsuboi, M., & Miyazaki, A. 1998, ApJS, 118, 455
Ozawa, H., Nagase, F., Ueda, Y., Dotani, T., & Ishida, M. 1999, ApJ, 523, L81
Pfahl, E., & Rappaport, S. 2000, ApJ, in press [astro-ph/0009212]
Predehl, P., & Schmitt, J. H. M. M. 1995, A&A, 293, 889
Sekimoto, Y., Matsuzaki, K., Kamae, T., et al. 2000, PASJ, 52, 31
Shepherd, D. S., & Kurtz, S. E. 1999, ApJ, 523, 690
Shiki, S., Ohishi, M., & Deguchi, S. 1997, ApJ, 478, 206
Sidoli, L. 2000, Ph.D. Thesis, University of Milan, Italy
Sidoli, L., Mereghetti, S., Israel, G. L., et al. 1999, ApJ, 525, 215
Sidoli, L., & Mereghetti, S. 1999, A&A, 349, L49
Sidoli, L., Mereghetti, S., Israel, G. L., & Bocchino, F. 2000, A&A, 361, 719
Sidoli, L., Belloni, T., & Mereghetti, S. 2001, A&A, 368, 835
Skibo, J. G., & Ramaty, R. 1993, A&AS, 97, 145
Sunyaev, R. A., Markevitch, M., & Pavlinsky, M. 1993, ApJ, 407, 606
Sunyaev, R. A., & Churazov, E. 1998, MNRAS, 297, 1279
Tanaka, Y., Miyaji, T., & Hasinger, G. 1999, Astron. Nachr., 320, 181
Tatischeff, V., Ramaty, R., & Kozlovsky, B. 1998, ApJ, 504, 874
Townes, C. H. 1989, in IAU Symp. 136, The Center of the Galaxy, ed. M. Morris (Dordrecht: Kluwer), 1
Treves, A., Turolla, R., Zane, S., & Colpi, M. 2000, PASP, 112, 297
Tsuboi, M., Handa, T., & Ukita, N. 1999, ApJS, 120, 1
Valinia, A., & Marshall, F. E. 1998, ApJ, 505, 134
Valinia, A., Tatischeff, V., Arnaud, K., et al. 2000, ApJ, in press
van Buren, D., et al. 1990, ApJ, 353, 570
van Paradijs, J. 1995, in X–ray Binaries, ed. W. H. G. Lewin, J. van Paradijs, & E. P. J. van den Heuvel (Cambridge Univ. Press), 536
Watson, M. G., Willingale, R., Grindlay, J. E., & Hertz, P. 1981, ApJ, 250, 142
Wilson, T. L., Ruf, K., Walmsley, C. M., et al. 1982, A&A, 115, 185
Yahel, R. Z. 1982, A&A, 109, 1
Yamauchi, S., & Koyama, K. 1993, ApJ, 404, 620
Yoshida, K., Inoue, H., & Osaki, Y. 1992, PASP, 44, 537
Zane, S., Turolla, R., & Treves, A. 1996, ApJ, 471, 248